Minimum inertia estimation of power-electronized power system considering multi-resource frequency response characteristics

Xia Zhou[1], Yishi Liu[1], Jianfeng Dai[1], Yi Tang (GE)[2], Tengfei Zhang[1], and Feng Xue[3]

[1]Nanjing University of Posts and Telecommunications
[2]Southeast University
[3]NARI Group (State Grid Electric Power Research Institute)

March 10, 2023

Abstract

With the large-scale grid connection of power electronic power sources, the power system gradually exhibits the characteristics of 'low inertia', and the indexes of frequency characteristics are getting closer to the safety critical value, which seriously affects the frequency safety of the system operation. To quantitatively analyze the minimum inertia requirement of the power electronic power system under the condition of multi-resource participation in frequency regulation (FR) when it is disturbed by active power, based on the improved frequency response model of the multi-machine system, this paper proposes a minimum inertia estimation method of the power system considering the frequency response characteristics. The theoretical inertia of each FR unit is represented in the form of rotor kinetic energy, and the calculated inertia of the power system is quantified based on the Rate of Change of Frequency (RoCoF). The sliding window technique is used to select the data set with the smallest variance and obtain the final calculated inertia of the system. The proposed estimation method takes the initial RoCoF, the maximum frequency deviation, and the steady-state frequency deviation as the frequency change constraint indicators, and adds the minimum inertia improvement measures to reduce the demand for the minimum inertia. Finally, the PSD-BPA software is used to verify the accuracy of the proposed model. And based on the improved frequency response model of the multi-machine system, MATLAB/Simulink is used to verify the proposed minimum inertia estimation method.

Minimum inertia estimation of power-electronized power system considering multi-resource frequency response characteristics

Xia Zhou [1], Yishi Liu [2], Jianfeng Dai [2], Tang Yi [3], Tengfei Zhang [2*], Feng Xue [4]

[1] Institute of Advanced Technology, Nanjing University of Posts and Telecommunications, Nanjing, China
[2] College of Automation & College of Artificial Intelligence, Nanjing University of Posts and Telecommunications, Nanjing, China
[3] School of Electrical Engineering, Southeast University, Nanjing, China
[4] NARI Group (State Grid Electric Power Research Institute), Nanjing, China
[*] tfzhang@126.com

Abstract: With the large-scale grid connection of power electronic power sources, the power system gradually exhibits the characteristics of 'low inertia', and the indexes of frequency characteristics are getting closer to the safety critical value, which seriously affects the frequency safety of the system operation. To quantitatively analyze the minimum inertia requirement of the power electronic power system under the condition of multi-resource participation in frequency regulation (FR) when it is disturbed by active power, based on the improved frequency response model of the multi-machine system, this paper proposes a minimum inertia estimation method of the power system considering the frequency response characteristics. The theoretical inertia of each FR unit is represented in the form of rotor kinetic energy, and the calculated inertia of the power system is quantified based on the Rate of Change of Frequency (RoCoF). The sliding window technique is used to select the data set with the smallest variance and obtain the final calculated inertia of the system. The proposed estimation method takes the initial RoCoF, the maximum frequency deviation, and the steady-state frequency deviation as the frequency change constraint indicators, and adds the minimum inertia improvement measures to reduce the demand for the minimum inertia. Finally, the PSD-BPA software is used to verify the accuracy of the proposed model. And based on the improved frequency response model of the multi-machine system, MATLAB/Simulink is used to verify the proposed minimum inertia estimation method.

1. INTRODUCTION

With the low-carbon transformation of the global energy structure, the power-electronized power system (PEPS) has developed rapidly. China proposes to achieve carbon neutrality by 2060 [1]. The EU plans to achieve a 32% penetration rate of new energy power generation by 2030 [2-3]. The United States predicts that the proportion of renewable energy will exceed 36% in 2050 [4]. Compared with the traditional synchronous power system, the power electronic power sources represented by wind power and high voltage direct current (HVDC) transmission in the PEPS are connected to the grid on a large scale [5-7]. However, due to the replacement of a high proportion of traditional synchronous inertia and the decoupling characteristics of power electronic power supplies [8], the inertia level of the power system is sharply reduced and the FR capability is relatively weakened, which will lead to a series of power system frequency operation safety problems [9-11]. Once a large active power disturbance occurs in the power grid (e.g. the disconnection of the tie line of the bulk power grid, the disconnection of the island operating unit, the fluctuation of the active power output of the power electronic power supplies, or the violent fluctuation of the active power on the load side), it is easy to trigger low-frequency load shedding or high-frequency cutting machine [12,13]. In recent years, the power system blackout accidents represented by South Australia '9.28' [14] and the United Kingdom "8.9" [15] are all related to the frequency instability caused by the lack of system inertia. When the power system inertia magnitude is lower than the minimum inertia demand, the power system frequency resilience collapses, resulting in system operational safety and stability problems. Therefore, it is of great significance to evaluate the minimum inertia of the PEPS based on improving the frequency characteristics of the system.

To compensate for the synchronous inertia possessed by the replaced synchronous generator, current power electronic-based power sources use frequency control techniques to simulate the synchronous inertia of the synchronous generator and provide a portion of the active power support for the power system [16-20]. On the source side of the power system, in the case of wind turbines, for example, the inertial response is made possible mainly through improvements to the converter or the addition of a frequency control unit [16]. On the other hand, considering that the wind turbine pitch angle adjustment ability is more potent, the inertial response control method is often added for active power modulation to alleviate the active power imbalance of the system, thereby improving the frequency safety and stability of the system operation [17]. For long-distance power transmission across regions, the system moment of inertia is split, so the system inertia of different regions cannot be shared [18]. In response to this, virtual synchronization technology is used in HVDC transmission [19, 20], and the inertia is provided by the DC capacitors in the converter stations on both sides. The supporting characteristics of the virtual inertia provided are similar to

those of the synchronous machine, which essentially realizes the function of primary FR active power modulation. The virtual inertia of the power electronic power supply makes the FR resources of the PEPS present a trend of diversification, and the primary FR capability is greatly improved.

However, due to the diversified development of system inertia support sources, the need for minimum inertia in power systems has changed accordingly. Therefore, the evaluation of minimum inertia under multi-source participation in FR in the PEPS needs urgent research in response to the requirements for safe and stable frequency operation. At present, there are relevant literatures to guide the minimum inertia estimation of power systems, which are mainly divided into two research directions. The first research direction is to use the real-time monitoring device to directly estimate the system inertia online, and collect the inertia data in real-time through the power grid online monitoring platform to grasp the inertia support capability of the system under normal and fault conditions [21-23]. Based on the collected large-scale inertial measurement data, the researchers use historical operating state experience to estimate the minimum inertia of the system. In [21], a synchrophasor measurement unit (PMU) is proposed to add to the bulk power grid transmission system and divide the power grid into different regions. According to the split power generation area, the inertia estimation is carried out at the regional level. Finally, the data is integrated and the overall inertia of the grid is estimated for the entire network. Given the safety requirements of phase angle operation under the high penetration rate of new energy sources, it is pointed out that the inertia can be estimated online through the PMU phase angle measurement data [22]. In addition, considering the error problem caused by the phase step, the aggregate inertia of the system is evaluated based on the law of conservation of angular momentum [23]. This study analyzes the flaws of PMUs for online inertia estimation and analyzes the system inertia in terms of the collected frequency variation. However, the calculation ideas in [21-23] are all based on the use of existing fixed grid architectures and data capture devices for calculation and evaluation. When the physical architecture of the grid is significantly altered from the traditional original architecture, or when the proportional approach to the combination of FR resources in the PEPS is unclear, the above methods for assessing and predicting inertia are not applicable.

Aiming at the problem of online monitoring of power system inertia in situation prediction, the second research direction of minimum inertia estimation is to estimate the minimum inertia of the system based on the frequency change characteristics. This research direction is based on the model analysis method, focusing on the analysis and prediction of the system inertia under the uncertain unit combination mode. In [24], it carried out the multi-machine aggregation of wind farms. The equivalent virtual inertia magnitude is estimated based on an improved frequency response model for wind turbine participation in the system with frequency regulation. However, this study only considers the wind farm station level, and cannot reflect the equivalent inertia situation of the power system under the diversified FR of asynchronous power sources. Based on the energy architecture environment with a high proportion of asynchronous power grids connected to the grid, a synchronous inertia constraint economic scheduling algorithm is proposed based on the RoCoF and frequency deviation constraints, and the minimum inertia demand of the system is calculated [25]. The optimization objective of this study is the financial cost of dispatching, so the critical inertia index is not the same as the frequency safety constraint, so it is not suitable for the minimum inertia estimation that only considers the frequency safety feature. In [26], considering the inertia drop problem caused by the decoupling characteristics of wind power converters, the minimum inertia of the system is quantitatively analyzed by the established system frequency response model under the condition of considering the minimum frequency constraint and the frequency change rate. However, this study only evaluates the minimum inertia for the power grid with fixed FR resources. It does not propose to optimize the minimum inertia demand under the consideration of frequency safety constraints. The model analysis method adopted in [24-26] can be used in the current PEPS with diversified FR resources. However, the FR resources models constructed in the above studies do not have the characteristics of the PEPS with multi-link interaction adjustment, and cannot achieve the minimum inertia evaluation under the participation of multiple FR resources in FR.

Given the above problems, this paper considers a PEPS FR control mode under the combined FR of thermal power, wind power, and HVDC transmission. The minimum inertia optimization adjustment strategy is considered in the minimum inertia estimation with the frequency operation safety characteristic as the constraint index. The rest of the paper is organized as follows. The second part establishes an improved frequency response model of the multi-machine system and quantitatively analyzes the frequency characteristics. The third part introduces the solution method of the theoretical inertia of each FR unit and proposes the solution method of the calculated inertia based on the frequency change rate. The fourth section describes the minimum inertia estimation method proposed in this paper. The fifth part is the simulation verification result based on MATLAB/Simulink and PSD/BPA platform. Section six concludes the article.

2. QUANTITATIVE ANALYSIS OF FREQUENCY CHARACTERISTICS OF THE POWER SYSTEM UNDER MULTI-RESOURCE FR

2.1. Power System Frequency Response Model

American scholar P. M. Anderson proposed the System Response Model (SFR) in 1990 [27], which reflects the power balance relationship between the source side and the load ends of the power system. With the development of PEPSs, the trend of multi-resource participation in joint FR ie power systems has become more prominent. The diversification of FR resources makes the single-machine equivalent SFR model unable to meet the quantitative analysis goals of the system. For bulk power grids, the multi-machine SFR model is used in this paper to reflect the frequency characteristics of the power system under multi-resource joint FR, as shown in Fig. 1.

F_{HPi} is the work ratio of the high-pressure cylinder of the i_{th} thermal power generator, T_{RHi} is the reheating time constant of the i_{th} thermal power generator, T_{Gi} is the time constant of the governor of the i_{th} thermal power generator,

T_{CHi} is the time constant of the steam box of the i_{th} thermal power generator, and R_i is the adjustment coefficient of the governor of the i_{th} thermal power generator; k_{dfq} is the inertia response coefficient of the q_{th} wind turbine, k_{pfq} is the primary FR coefficient of the q_{th} wind turbine, $T_{\beta q}$ is the response time constant of the q_{th} wind turbine pitch angle change, and $T_{\omega q}$ is the rotor inertia response time constant of the q_{th} wind turbine; α_j is the droop control coefficient of the j_{th} HVDC transmission, T_{DCj} is the inertia link time constant of the j_{th} HVDC transmission; ΔP_R, ΔP_{DC} and ΔP_{WF} are the variation of active power of traditional thermal power FR unit, HVDC FR unit and wind turbine FR unit respectively; ρ_R , ρ_{DC} and ρ_{WF} are the FR coefficients of traditional thermal power FR units, HVDC FR units, and wind turbine FR units, respectively, that is, the ratio of the FR active power of each FR unit to the total FR active power; $\Delta f(s)$ is the frequency variation; $\Delta P_L(s)$ is the load active power disturbance ; H_{sys} and D_{sys} are the equivalent time constant and damping coefficient of the system, respectively; s is the frequency domain differential operator.

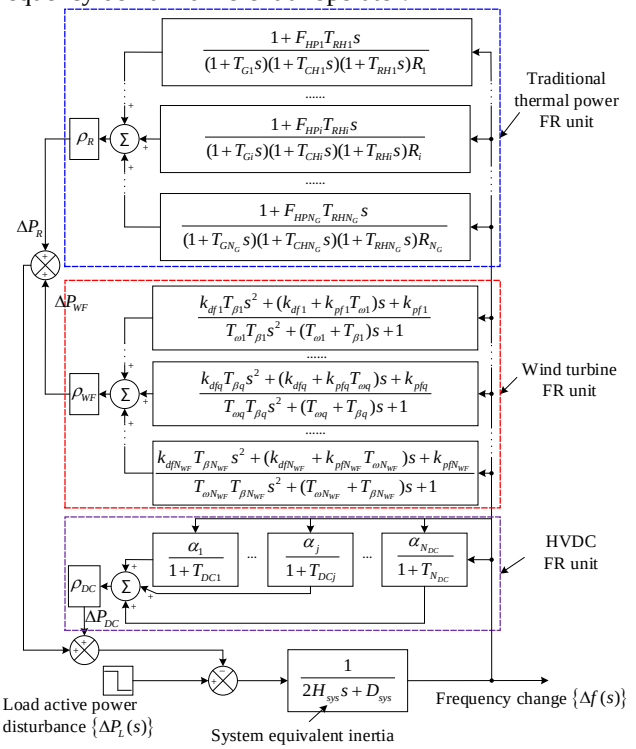

Fig. 1 Frequency response model of the multi-machine system

2.2. Quantitative Analysis of Frequency Characteristics of Power System

This section establishes the rotor motion equation according to the frequency response model of the multi-machine system in Section 2.1, and quantitatively analyzes the frequency variation of the power system under the unit active power disturbance through the rotor motion equation, that is, quantitatively analyzes the power system frequency characteristic transfer function. The frequency characteristic of the power system is calculated based on the frequency characteristic transfer function. It can be seen from Fig. 1 that when the load active power disturbance occurs in the power system, the equation of motion of the system rotor is:

$$2H_{sys}\frac{d\Delta f(t)}{dt}+D_{sys}\Delta f(t)=-\Delta P_L(t)-\Delta P_R(t)-\Delta P_{DC}(t)-\Delta P_{WF}(t) \quad (1)$$

Converting (1) into frequency domain form using the *Laplace* transform formula:

$$\left[-\Delta P_L(s)-\Delta P_R(s)-\Delta P_{DC}(s)-\Delta P_{WF}(s)\right]\cdot\frac{1}{2H_{sys}s+D_{sys}}=\Delta f(s) \quad (2)$$

According to (2), when multiple resources participate in FR, the frequency variation of the power system is related to the FR power of each FR unit, the power disturbance of the load, the system equivalent inertia time constant, and the equivalent damping. Among them, the FR active power of each FR unit depends on the FR control strategy of the power system, and the equivalent inertia of the PEPS is related to the FR control strategy. Therefore, it is necessary to analyze the influence of specific FR control parameters on the frequency characteristics of the power system, and then quantitatively analyze the relationship between inertia and frequency characteristics.

To characterize the influence of each FR unit on the frequency characteristics of the power system, (2) can be expressed as:

$$\begin{aligned}&-\Delta P_L(s)-\rho_R\cdot\mathrm{A}\cdot\Delta f(s)-\rho_{DC}\cdot\mathrm{B}\cdot\Delta f(s)-\rho_{WF}\cdot\mathrm{C}\cdot\Delta f(s)\\&=(2H_{sys}s+D_{sys})\cdot\Delta f(s)\end{aligned} \quad (3)$$

where A, B, and C are polynomials with respect to the frequency-domain differential operators and meet the conditions:

$$\begin{cases}\mathrm{A}=\sum_{i=1}^{N_G}\dfrac{1+F_{HPi}T_{RHi}s}{(1+T_{Gi}s)(1+T_{CHi}s)(1+T_{RHi}s)R_i}\\ \mathrm{B}=\sum_{j=1}^{N_{DC}}\dfrac{\alpha_j}{1+sT_{DCj}}\\ \mathrm{C}=\sum_{q=1}^{N_{WF}}\dfrac{k_{dfq}T_{\beta q}s^2+(k_{dfq}+k_{pfq}T_{\omega q})s+k_{pfq}}{T_{\omega q}T_{\beta q}s^2+(T_{\omega q}+T_{\beta q})s+1}\end{cases} \quad (4)$$

In order to investigate the frequency variation of the power system under power disturbance, the frequency characteristic transfer function of the power system $G_{sys}(s)$ is defined as:

$$G_{sys}(s)=\frac{\Delta f(s)}{-\Delta P_L(s)} \quad (5)$$

From (4) and (5), the frequency characteristic transfer function of the power system under multi-resource FR can be obtained:

$$G_{sys}(s)=\frac{\Delta f(s)}{-\Delta P_L(s)}=\frac{1}{\rho_R\cdot\mathrm{A}+\rho_{DC}\cdot\mathrm{B}+\rho_{WF}\cdot\mathrm{C}+2H_{sys}s+D_{sys}} \quad (6)$$

The initial RoCoF, S_0, which is calculated by the initial value theorem (Equation (7)) when the power system is disturbed by active power under multi-resource FR, is shown in (8):

$$S_0=\lim_{t=0^+}\frac{d\Delta f(t)}{dt}=\lim_{s=+\infty}s^2\Delta f(s)=\lim_{s=+\infty}s^2G_{sys}(s)\frac{-\Delta P_L}{s} \quad (7)$$

$$S_{0\_sys}=\frac{-\Delta P_L}{2H_{sys}} \quad (8)$$

where S_{0_sys} is the per-unit value of the initial RoCoF of the system.

According to (8), when the power system is subjected to a certain amount of active power disturbance (the active power imbalance between the source side and the load side is known), the absolute value of the system's initial RoCoF is inversely proportional to the system equivalent inertia. Different from the classical SFR model that only considers the primary FR of thermal power, the equivalent inertia of the traditional model is only related to the inertia time constant of the thermal power unit in the system. However, the equivalent inertia of the PEPS also involves the virtual inertia provided by the power electronic power supply, which will be analyzed in Chapter 3.

The final value theorem (Equation (9)) is used to calculate the steady-state frequency deviation of the power system under this FR strategy, and the result is shown in (10):

$$\Delta f_{ss} = \lim_{s\to 0} s \cdot G_{sys}(s) \cdot \frac{-\Delta P_L}{s} \tag{9}$$

$$\Delta f_{ss\_sys} = \frac{-\Delta P_L}{\rho_R \cdot \sum_{i=1}^{N_G} \frac{1}{R_i} + \rho_{DC} \cdot \sum_{j=1}^{N_{DC}} \alpha_j + \rho_{WF} \cdot \sum_{q=1}^{N_{WF}} k_{pfq} + D_{sys}} \tag{10}$$

where Δf_{ss_sys} is the steady-state frequency deviation of the power system. Assuming that the FR units of the same type of FR units have the same capacity, and the multi-machine system frequency response models are aggregated into an equivalent system frequency response model, (10) can be transformed into:

$$\Delta f_{ss\_sys} = \frac{-\Delta P_L}{\rho_R \cdot \frac{N_G}{R} + \rho_{DC} \cdot \alpha N_{DC} + \rho_{WF} \cdot k_{pf} N_{WF} + D_{sys}} \tag{11}$$

where R, α, and k_{pf} are the equivalent differential adjustment coefficient of the governor of the thermal power generator, the droop coefficient of HVDC transmission, and the primary frequency adjustment coefficient of the wind turbine under the aggregation of the multi-machine model, and the parameters satisfy:

$$\frac{1}{R} = \frac{1}{N_G} \cdot \sum_{i=1}^{N_G} \frac{1}{R_i}, \quad \alpha = \frac{1}{N_{DC}} \cdot \sum_{j=1}^{N_{DC}} \alpha_j, \quad k_{pf} = \frac{1}{N_{WF}} \cdot \sum_{q=1}^{N_{WF}} k_{pfq} \tag{12}$$

Assuming that all power generation units in a certain system participate in FR, the relationship between the absolute value of steady-state frequency deviation and the active power disturbance of the load and the FR coefficient of traditional thermal power is drawn based on (11), as shown in Fig. 2. The parameter settings are as following: N_G=N_{DC}=N_{WF}=1, R=0.05, ρ_{DC}=0.2, α=8, k_{pf}=20, D_{sys}=2, and ρ_R+ρ_{DC}+ρ_{WF}=1.

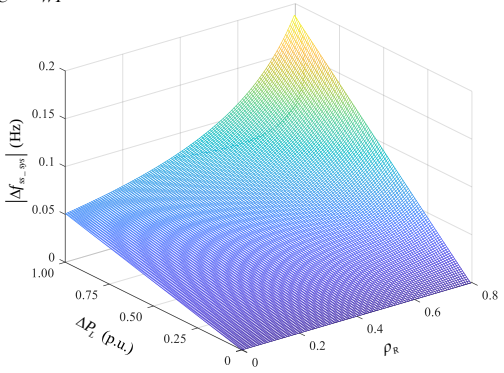

Fig. 2 Steady-state frequency characteristic factor influence diagram

According to (11), assuming that the rated capacity of the same type of FR units is the same when the frequency of the power system tends to be stable, the steady-state frequency deviation is related to the FR control parameters, the FR coefficient and the number of FR units, which is irrelated to the equivalent time constant of inertia of the system. However, it can be seen from Fig. 2 that when all units participate in FR, the larger the active power disturbance of the load and the traditional thermal power FR coefficient, the larger the absolute value of the steady-state frequency deviation and the more unstable the steady-state frequency characteristics, that is, the support ability of equivalent inertial of the system is worse. Therefore, under the actual power grid operation, different FR coefficients (ρ_R, ρ_{DC}, and ρ_{WF} are different) determine the connection of FR units of various capacities, resulting in various system equivalent FR capacities and thus other system equivalent inertias. Therefore, the inertia research of the power system needs to combine the multi-resources to participate in the analysis of the frequency characteristics of the power system under FR.

3. INERTIA THEORY CONSIDERING FREQUENCY RESPONSE CHARACTERISTICS

The inertia of the power system is manifested as a resistance to the imbalance between the active power support and the load power demand caused by external power disturbances, preventing the large fluctuation of the grid frequency. It is an essential guarantee for maintaining the system's frequency stability. Because of the complexity of the frequency response characteristics of the power system under multi-resource participation in FR, the system inertia is expressed in the form of energy.

3.1. Theoretical inertia

Inertia is defined as the ability of a power system to resist frequency changes [28]. For a single generator, the theoretical value of inertia represents the rotor kinetic energy of the generator at the rated angular speed, the unit is MW·s, and the expression is:

$$E_{Gi} = H_i S_i = \frac{1}{2} J_i \omega_n^2 \tag{13}$$

where E_{Gi}, H_i, S_i, J_i, ω_n are the theoretical inertia value, inertia time constant, capacity, rotational inertia, and rotor-rated angular speed of the i_{th} generator, respectively.

In a multi-generator power system with only conventional synchronous generator sets, the theoretical value of the system equivalent inertia is the sum of the generator inertias in the system:

$$E_G = \sum_{i\in T} E_{Gi} = \sum_{i\in T} H_i S_i \tag{14}$$

where E_G is the equivalent theoretical inertia of the system, and T is the set of conventional synchronous generators.

With the rapid development of PEPSs, the grid connection of power electronic power sources makes the level of inertia of the power system decrease continuously. To deal with the instability of the system frequency caused by the reduction of the inertia level, the new energy adopts the virtual inertia control technology, and the HVDC

transmission line adopts the virtual synchronous machine control technology. Therefore, the equivalent inertia of the PEPS under the multi-resource participation in FR is provided by the synchronous inertia of the synchronous generator and the virtual inertia of the new energy and HVDC transmission. The theoretical value of the equivalent inertia of the PEPS is shown in (15):

$$\begin{aligned} E_{sys} &= E_{TR} + E_{WF} + E_{HVDC} \\ &= \sum_{i=1}^{N_G} H_{Ri} S_{Ri} Z_{Ri} + \sum_{q=1}^{N_{WF}} H_{WFq} S_{WFq} Z_{WFq} + \sum_{j=1}^{N_{DC}} H_{DCj} S_{DCj} Z_{DCj} \end{aligned} \quad (15)$$

where E_{TR}, H_{Ri}, S_{Ri}, and Z_{Ri} are the inertia of traditional thermal power, the inertia time constant, capacity, and start-stop status of the i_{th} thermal power unit; E_{WF}, H_{WFq}, S_{WFq}, and Z_{WFq} are the virtual inertia provided by the new energy wind turbine, the virtual inertia time constant, capacity and start-stop status of the q_{th} typhoon wind turbine; E_{HVDC}, H_{DCj}, S_{DCj}, and Z_{DCj} are the inertia provided by the HVDC virtual synchronous machine, the inertia time constant of the j_{th} HVDC virtual synchronous machine, DC converter station capacity, and start-stop status.

From (15), the equivalent inertia time constant of the PEPS can be obtained as:

$$H_{sys} = \frac{\sum_{i=1}^{N_G} H_{Ri} S_{Ri} Z_{Ri} + \sum_{q=1}^{N_{WF}} H_{WFq} S_{WFq} Z_{WFq} + \sum_{j=1}^{N_{DC}} H_{DCj} S_{DCj} Z_{DCj}}{\sum_{i=1}^{N_G} S_{Ri} Z_{Ri} + \sum_{q=1}^{N_{WF}} S_{WFq} Z_{WFq} + \sum_{j=1}^{N_{DC}} S_{DCj} Z_{DCj}} \quad (16)$$

3.2. Calculated inertia

When the power system is disturbed by the active power of the load, the traditional synchronous generator set, the wind generator set using the inertial response control technology, and the HVDC virtual synchronous generator converter station release energy to compensate for the power imbalance between the power grid source and the load. Taking a single generator ζ as an example, the calculated inertia based on the frequency response characteristics is

$$E_{C\zeta} = H_\zeta S_\zeta = \frac{\omega_n^2 \Delta P_\zeta}{2\omega_\zeta \frac{\mathrm{d}\omega_\zeta}{\mathrm{d}t}} = \frac{\omega_n^2 (P_{m\zeta} - P_{e\zeta})}{2\omega_\zeta \frac{\mathrm{d}\omega_\zeta}{\mathrm{d}t}} \quad (17)$$

where $E_{C\zeta}$ is the calculated inertia value of generator ζ; ω_n is the rated angular frequency; ω_ζ is the angular frequency of generator ζ; ΔP_ζ is the vacancy of the active power of generator ζ; $P_{m\zeta}$ is the mechanical power of generator ζ; $P_{e\zeta}$ is the electromagnetic power of generator ζ.

Extending the calculated inertia of a single generator to a new type of power system with multiple generators ($\omega_n = \omega_\zeta$)[29], the equivalent calculated inertia of the power system is expressed as

$$E_{Csys} = H_{Csys} S_{sys} = \frac{f_n \Delta P}{2\frac{\mathrm{d}f_{sys}}{\mathrm{d}t}} \quad (18)$$

where E_{Csys} is the equivalent calculated inertia value of the power system; S_{sys} is the sum of the capacity of the power system; ΔP is the vacancy of the active power of the entire power system; f_{sys} is the frequency at the moment when a certain node disturbance occurs. Where,

$$S_{sys} = \sum_{i=1}^{N_G} S_{Ri} Z_{Ri} + \sum_{q=1}^{N_{WF}} S_{WFq} Z_{WFq} + \sum_{j=1}^{N_{DC}} S_{DCj} Z_{DCj} \quad (19)$$

From (18), it can be seen that the inertia estimation needs to collect the initial RoCoF of a certain system node at the time of disturbance. Therefore, an inaccurate measurement of the RoCoF at the time of acquisition will lead to an increase in inertia estimation error. On the other hand, due to the inconsistent time scale of inertia response and primary FR, the data measurement error of a single time node is large.

To reduce the calculation error of inertia estimation, the data processing technology based on the sliding window is adopted when calculating the inertia of the power system. When the primary FR is involved, the unbalance of the active power between the source side and the load side of the grid is compensated by the inertia response and the primary FR response simultaneously. By sampling data parameters at two different times, the traditional method of evaluating the RoCoF of a single node is replaced. t_1 is the time point when the disturbance occurs, and t_2 is the sampling time point. Since the inertia values of the power system at different sampling times t_2 are different, an equivalent inertia curve of the power system that changes with the sampling time can be drawn. Based on the sliding window technology, the time interval with the smallest fluctuation on the curve is selected, and the sampling value is calculated to obtain the average value of the time interval. The inertia estimation results are as follows:

$$S^2 = \frac{\sum_{t_n=\tau}^{\upsilon} (E_{t_2=t_n} - \overline{E})}{\upsilon} \quad (20)$$

$$\min S^2 = \min \left\{ \frac{\sum_{t_n=\tau}^{\upsilon'} (E_{t_2=t_n} - E_{Csys}')^2}{\upsilon'} \right\} \quad (21)$$

$$E_{Csys}' = \frac{\sum_{t_n=\tau}^{\upsilon'} E_{t_2=t_n}}{\upsilon'} \quad (22)$$

where $\overline{E}$ is the average value of inertia in the sampling interval; v is the number of data in the sampling interval; $E_{t_2=t_n}$ is the calculated inertia value when t_2 is equal to t_n at the sampling time; τ is the initial sampling time of the current time interval; E_{Csys}' is the equivalent inertia value of the system; v' is the number of valid sampling time interval data.

4. MINIMUM INERTIA ESTIMATION OF POWER SYSTEM CONSIDERING FREQUENCY RESPONSE CHARACTERISTICS

The frequency characteristics of the PEPS under the multi-resource participation in FR directly reflect the support capability of its synchronous inertia and asynchronous inertia. This section introduces the minimum inertia estimation method under the constraint of the RoCoF and frequency deviation and considers the optimization measures of FR control parameters to reduce the minimum inertia demand of the system. The final minimum inertia of

the power system is obtained taking into account the frequency response characteristics.

4.1. Minimum inertia estimation considering RoCoF constraint

The maximum RoCoF should be used as the parameter benchmark if the RoCoF does not exceed a certain critical value after the power system is disturbed.

According to (1), when the active power is unbalanced, there is no frequency deviation in the power system at this moment because it is at the moment of disturbance. The frequency variation of the power system depends on the system's equivalent inertia time constant and the active power disturbance.

The minimum inertia of the power system based on RoCoF constraint is

$$H_{\text{min\_RoCoF}} = \frac{\Delta P_{\max}}{2\,\text{RoCoF}_{\max}} \tag{23}$$

It means that when the system is subjected to the maximum active power disturbance $\Delta P_{\max}$, in order to make the central RoCoF not exceed the critical value $\text{RoCoF}_{\max}$, the inertia of the system after the disturbance must not be smaller than $H_{\min}$.

Since the maximum RoCoF is the initial RoCoF, (23) can be expressed as

$$H_{\text{min\_RoCoF}} = \frac{\Delta P_{\max}}{2S_{0\_sys}} \tag{24}$$

Then the minimum inertia estimation value under the actual power system is

$$H_{\text{min\_RoCoF}}' = \frac{50\cdot\Delta P_{\max}}{2S_{0\_sys}} = \frac{25\Delta P_{\max}}{S_{0\_sys}} \tag{25}$$

According to (24), it can be known that the greater the active power imbalance between the source side and the load side, or the smaller $\text{RoCoF}_{\max}$, the greater the minimum inertia constraint of the power system, and the smaller the system inertia. From (25), the relationship between the minimum inertia demand of the power system and the magnitude of the active power disturbance and the initial RoCoF can be obtained, as shown in Fig. 3.

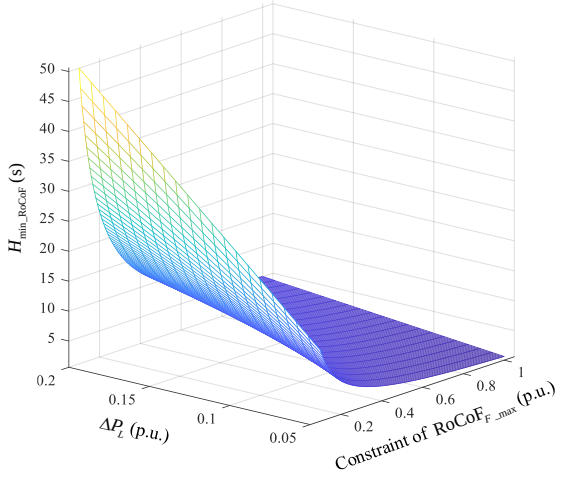

Fig. 3 Minimum inertia requirement under RoCoF constraints

4.2. Minimum inertia estimation considering frequency deviation constraints

The frequency characteristics of power systems under various power grid architectures are different. Therefore, in order to prevent large power outages caused by Under Frequency Load Shedding (UFLS) actions when the power grid is subjected to large disturbances, the system inertia support capability needs to consider the power grid frequency characteristics under multi-resource participation in FR. Taking China's power grid as an example, when traditional thermal power, wind turbines, and HVDC transmission jointly participate in FR, the lowest point of the grid frequency must not be lower than the action value of UFLS in the third defense line of the power grid, that is, the absolute value of the maximum frequency deviation $\Delta f_{\max}$ of the power system under the multi-resource participation FR does not exceed 1 Hz (abnormal operation state). When the frequency curve tends to be stable, the steady-state frequency characteristics reflect the system inertia characteristics during normal operation in the later stage of FR, and the absolute value of the grid steady-state frequency deviation Δf_{ss} should not exceed 0.2 Hz. Therefore, the minimum inertia of the power system considering the frequency deviation constraint can take the larger value of the minimum inertia that meets the above two conditions:

$$H_{\min}^{\Delta f} = \max\left\{H_{\min}^{\Delta f_{\max}}, H_{\min}^{\Delta f_{ss}}\right\} \tag{26}$$

When the power grid under safe and stable operation is disturbed later, the influence of the spatial distribution characteristics of the power grid is weakened. Therefore, based on the classical SFR model, the frequency response model of the power grid under the multi-resource participation FR is established, and the equivalent inertia of the power system under the constraint of the maximum frequency deviation is quantitatively studied. According to the principle of aggregation equivalence, the frequency response model of the multi-machine system in Fig. 1 is aggregated and equivalent. Fig. 4 is the frequency response model of the power system under the condition of multi-resource participation in FR after equivalence.

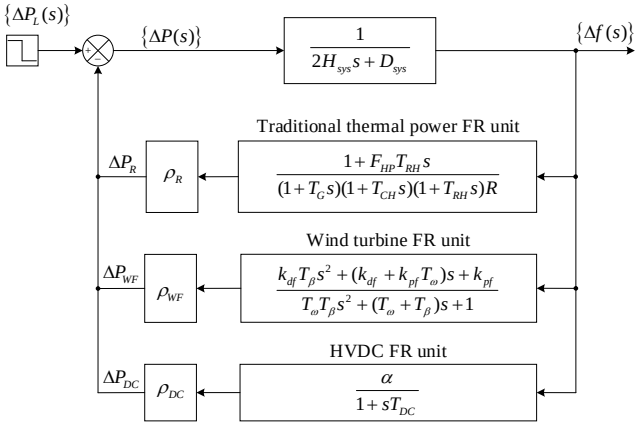

Fig. 4 Equivalent system frequency response model

Using the principle of aggregation equivalence, the parameters of each FR unit meet:

$$J = \frac{1}{N_\phi}\cdot\frac{\sum_{i=1}^{N_\phi} J_{\phi i}\cdot S_{\phi i}}{\sum_{i=1}^{N_\phi} S_{\phi i}} \tag{27}$$

where J represents the equivalent parameter factor after system aggregation; ϕ represents the category of FR units,

including traditional thermal power, wind power, and HVDC transmission; N_ϕ represents the number of units corresponding to the category of FR units; $J_{\phi i}$ is the parameter of the i_{th} ϕ-FR unit before aggregation; $S_{\phi i}$ is the capacity of the i_{th} ϕ-FR unit before the aggregation.

The traditional power system only considers the primary FR of thermal power, and its internal power electronic power supply does not participate in the primary FR. Therefore, the traditional analysis method of frequency characteristics based on the improved SFR model considers that the system equivalent inertia time constant is only related to the primary FR of thermal power, and has nothing to do with the combination of system FR resources. However, compared with the different sources of inertia in traditional power systems, the diversification of FR resources enables power electronic power supplies to participate in FR and provide certain virtual inertia support, and the capacity of the units participating in FR affects the equivalent inertia of the system in real-time.

Fig. 5 is the frequency curve under different parameter combinations, in which the active power disturbance of the load is set as ΔP_L = 0.06 p.u., and the other parameters are shown in the attached Tab A. It can be seen from Fig. 5(a) that when the influence of the unit combination mode on the equivalent inertia of the power system is not considered and the thermal power FR coefficient is unchanged, the increase of the wind power FR coefficient makes the time $t_{\max}$ for the power system to reach the maximum frequency deviation earlier. It can be seen from Fig. 5(b) that when the equivalent inertia of the system and the thermal power FR coefficient are changed in the same direction, the increase of the wind power FR coefficient also makes the time $t_{\max}$ of the maximum deviation of the system arrival frequency earlier. Still, the frequency characteristics of the two are pretty different. Therefore, the inertia estimation considering the FR constraint under the PEPS needs to consider the influence of the FR output of each FR unit on the equivalent inertia of the system.

4.3. Source-load-side response measures to deal with insufficient minimum inertia of the system

According to (1), the frequency characteristics of the power system under the multi-resource participation in FR depend on the equivalent inertia time constant of the system, the system equivalent load damping coefficient, the disturbance of the active power of the load, the primary FR power of conventional units and the FR active power of other FR units. Therefore, for the estimation of the minimum inertia of the PEPS considering the frequency characteristics, if the system inertia is insufficient (the sum of the system synchronous inertia and the virtual inertia is less than the minimum inertia requirement), in addition to increasing the system equivalent inertia time constant, it can also reduce the maximum disturbance of active power, the conventional primary FR control parameters, power electronic power supply FR control parameter, and adjust frequency constraints, as shown in Fig. 6.

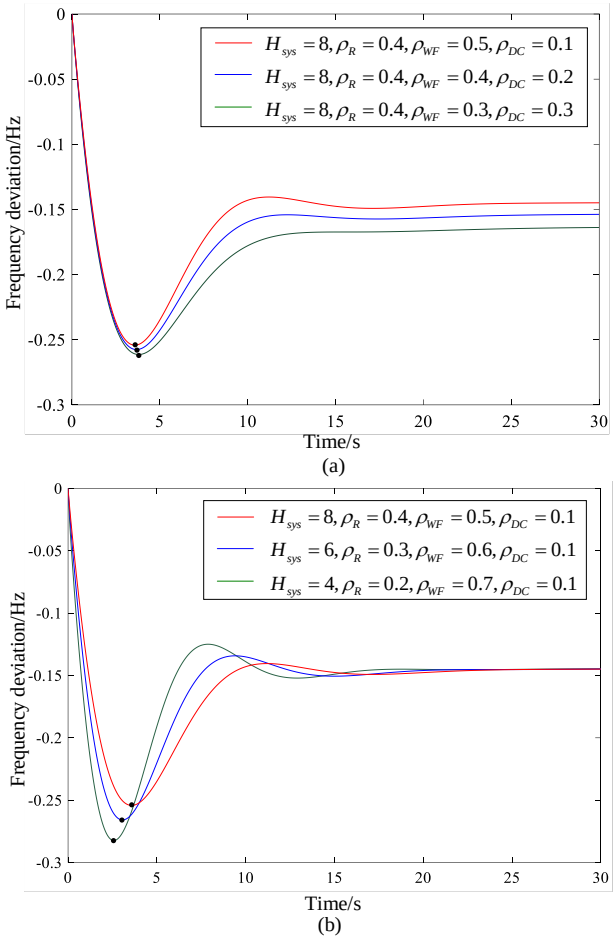

Fig. 5 System frequency characteristic curves: (a) The relationship between the equivalent inertia and the unit combination is not considered, (b) The equivalent inertia of the system and the thermal power FR coefficient change in the same direction

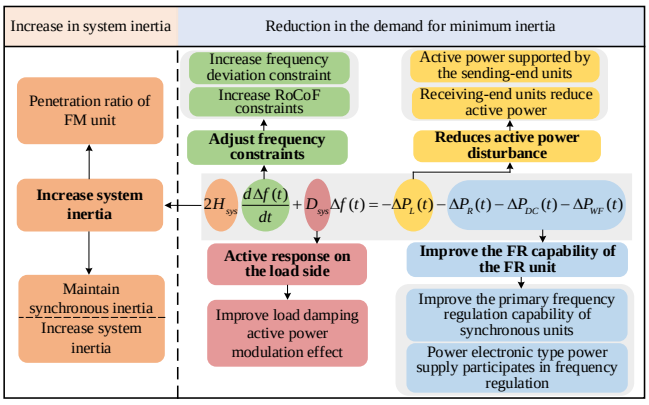

Fig. 6 Measures for insufficient minimum inertia of the system

4.3.1 Increase in system inertia

The penetration rate of new energy in traditional power systems is low, and the inertia in the system is mainly provided by synchronous generators and is relatively abundant. When the inertia of the traditional power system is insufficient, the system inertia level can be improved by adding synchronous units, and the grid-connected new energy units have almost no FR capability. However, the penetration rate of power electronic power sources represented by new energy and HVDC transmission in the PEPS under the dual-carbon goal is gradually increasing, and the inertia support capacity under the traditional FR

method can no longer meet the needs of operational safety. Therefore, based on maintaining the traditional inertia, it is necessary to combine the synchronous inertia with the virtual inertia of the power electronic type power supply.

In terms of maintaining the synchronous inertia, it is possible to add a synchronous condenser based on the current grid-connected traditional synchronous generator or change a retired thermal power plant to a synchronous condenser, and it is necessary to consider the economic factors of grid operation. In terms of increasing virtual inertia, it is mainly divided into voltage source type and current source type. The current source type has a simple structure but has a short delay (100 ms). The voltage source virtual inertia has a complex structure and high cost, but it can provide inertia support without delay. Therefore, considering factors such as operating communication delay and safety, current researchers are more inclined to increase the virtual inertia of the voltage source type. The penetration rate of power electronic power sources has increased, and in theory, power electronic power sources can completely replace traditional synchronous generators. Compared with the traditional synchronous inertia single support mode, the inertia support research of multi-resource participation in FR of the PEPS can be traced back to the change in the penetration rate of each FR unit. Therefore, according to the operating environment and operating requirements of the power grid in different regions, the minimum inertia of the power grid can be directly improved according to the combined adjustment of the penetration rate of multiple resources.

4.3.2 Reduction in the maximum disturbance of active power

This section takes the constraint on the initial RoCoF as an example. According to Section 4.1, it can be known that the demand for minimum inertia of the power system is proportional to the maximum disturbance of active power. Therefore, reducing the maximum disturbance of active power can reduce the demand for the minimum inertia, thus meeting the grid's demand for the system's support capability of equivalent inertia. The minimum inertia and maximum disturbance of active power are shown in Fig. 7. According to Fig. 7, it can be seen that when the constraint on the initial RoCoF is constant, if the maximum active power disturbance increases, the demand for minimum inertia of the system decreases. Therefore, when the minimum inertia of the system is insufficient, the maximum active power disturbance of the power grid can be reduced.

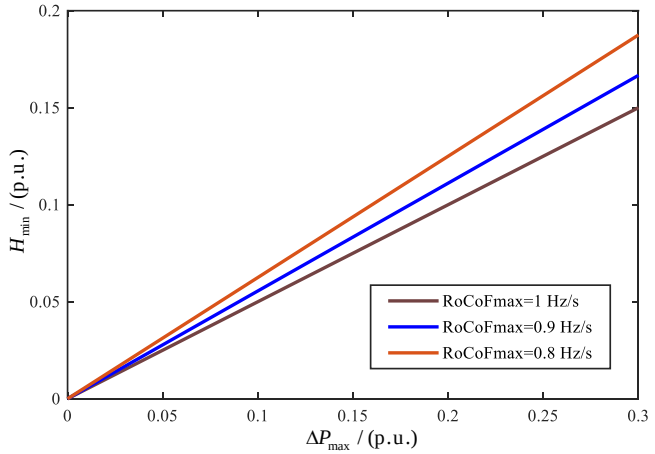

Fig. 7 The relationship between the minimum inertia and the maximum active power disturbance $\Delta P_{\max}$ of the power system

4.3.3 Adjustment of the primary FR control parameters

The frequency characteristics of the power system under multi-resource participation in FR reflect the compensation ability of the system's equivalent inertia to the unbalanced active power between the source side and the load side. According to (6), the frequency expression of the power system can be obtained as:

$$\Delta f(s)=\frac{-\Delta P_L(s)}{\rho_R\cdot \mathrm{A}+\rho_{DC}\cdot \mathrm{B}+\rho_{WF}\cdot \mathrm{C}+2H_{sys}s+D_{sys}} \tag{28}$$

From (4), it can be known that the polynomials A, B, and C do not contain the system equivalent damping coefficient D_{sys}, but the polynomial A contains the adjustment coefficient R, then the partial derivative of the frequency is obtained:

$$\frac{\partial \Delta f(s)}{\partial D}=\frac{\Delta P_L(s)}{(\rho_R\cdot \mathrm{A}+\rho_{DC}\cdot \mathrm{B}+\rho_{WF}\cdot \mathrm{C}+2H_{sys}s+D_{sys})^2} \tag{29}$$

$$\frac{\partial \Delta f(s)}{\partial R}=\frac{\partial \Delta f(s)}{\partial \mathrm{A}}\cdot\frac{\partial \mathrm{A}}{\partial R}= \frac{\left\{\rho_R\cdot\Delta P_L(s)\cdot\sum_{i=1}^{N_G}\frac{-(1+T_{Gi}s)(1+T_{CHi}s)(1+T_{RHi}s)(1+F_{HPi}T_{RHi}s)}{[(1+T_{Gi}s)(1+T_{CHi}s)(1+T_{RHi}s)R_i]^2}\right\}}{(\rho_R\cdot \mathrm{A}+\rho_{DC}\cdot \mathrm{B}+\rho_{WF}\cdot \mathrm{C}+2H_{sys}s+D_{sys})^2} \tag{30}$$

From (28) (29) (30) can know that the power system frequency is related to the system equivalent damping and adjustment coefficient, and the power system frequency variation can be determined by the system equivalent damping and adjustment coefficient.

Taking the steady-state frequency deviation constraint as an example, the partial derivative of (11) can be obtained:

$$\frac{\partial \Delta f_{ss\_sys}}{\partial R}=\frac{-\rho_R N_G\cdot\Delta P_L}{R^2\left(\rho_R\cdot\frac{N_G}{R}+\rho_{DC}\cdot\alpha\cdot N_{DC}+\rho_{WF}\cdot k_{pf}\cdot N_{WF}+D_{sys}\right)^2} \tag{31}$$

$$\frac{\partial \Delta f_{ss\_sys}}{\partial D_{sys}}=\frac{\Delta P_L}{\left(\rho_R\cdot\frac{N_G}{R}+\rho_{DC}\cdot\alpha\cdot N_{DC}+\rho_{WF}\cdot k_{pf}\cdot N_{WF}+D_{sys}\right)^2} \tag{32}$$

According to (31) and (32), it can be known that since $\Delta P_L>0$ is set in this paper, then $\partial\Delta f_{ss\_sys}/\partial R<0$, and $\partial\Delta f_{ss\_sys}/\partial D_{sys}>0$. Therefore, increasing the adjustment coefficient R and the system equivalent damping coefficient D_{sys} is beneficial to reduce the steady-state frequency error, thereby improving the system frequency stability. As shown in Fig. 8, it is the factor diagram of the conventional primary frequency modulation of the power system when the minimum inertia is insufficient.

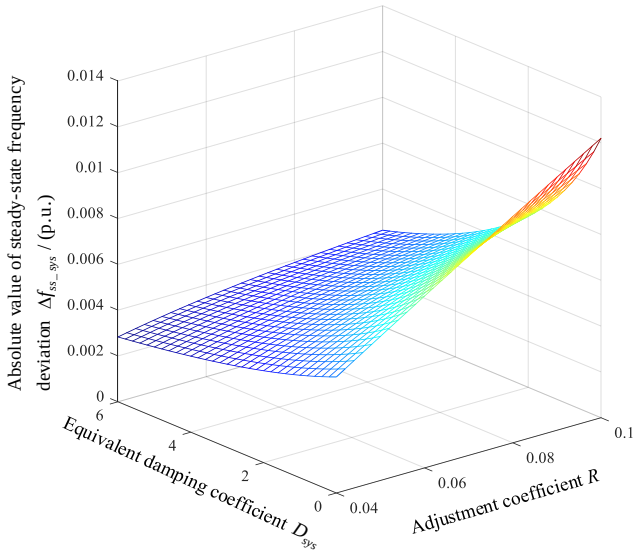

Fig. 8 Diagram of conventional primary FR factors of power system when the minimum inertia is insufficient

The FR capability of the synchronous unit and the response characteristics of the load ensure the balance of active power at both ends of the source side and the load side in the conventional sense, and its essence provides certain inertia support for the damping of the synchronous unit and the load end, thereby improving the FR capability of the power system. Therefore, the problem of insufficient minimum inertia of the power grid can be solved by adjusting the adjustment coefficient R of the synchronous unit and the system equivalent load damping D_{sys}.

4.3.4 Adjustment of the parameters of power electronic power supply FR control

The power electronic power supply participates in the FR of the power system by adding additional frequency control links. Therefore, it is helpful to analyze the FR control measures when the system inertia is insufficient under the multi-resource participation in FR by examining the related additional frequency control coefficients of new energy wind turbines and HVDC transmission.

Section 4.3.3 proposes that the steady-state characteristics of frequency can directly reflect the influence of the power system FR control parameters on the system frequency characteristics. Taking the steady-state frequency deviation constraint as an example, the partial derivative of (11) is obtained. The quantitative relationship between the primary FR coefficient of the wind turbines, the droop coefficient of HVDC transmission, and the frequency characteristics is investigated:

$$\frac{\partial \Delta f_{ss\_sys}}{\partial k_{pf}} = \frac{\rho_{WF} N_{WF} \cdot \Delta P_L}{\left(\rho_R \cdot \frac{N_G}{R} + \rho_{DC} \cdot \alpha \cdot N_{DC} + \rho_{WF} \cdot k_{pf} \cdot N_{WF} + D_{sys}\right)^2} \quad (33)$$

$$\frac{\partial \Delta f_{ss\_sys}}{\partial \alpha} = \frac{\rho_{DC} N_{DC} \cdot \Delta P_L}{\left(\rho_R \cdot \frac{N_G}{R} + \rho_{DC} \cdot \alpha \cdot N_{DC} + \rho_{WF} \cdot k_{pf} \cdot N_{WF} + D_{sys}\right)^2} \quad (34)$$

In this paper, it is assumed that the active power disturbance satisfies the condition $\Delta P_L>0$. According to (33) and (34), it can be known that $\partial \Delta f_{ss\_sys}/\partial k_{pf} >0$ and $\partial \Delta f_{ss\_sys}/\partial \alpha>0$. That is to say, increasing the primary FR coefficient k_{pf} of the wind turbine or the drooping coefficient α of the HVDC transmission can improve the frequency steady-state characteristics of the power system.

The influence of FR control parameters of the power electronic power supply on the frequency characteristics of the system is shown in Fig. 9(ΔP_L=0.1 p.u., D_{sys}=0, R=0.05, H_{sys}=2.445 s).

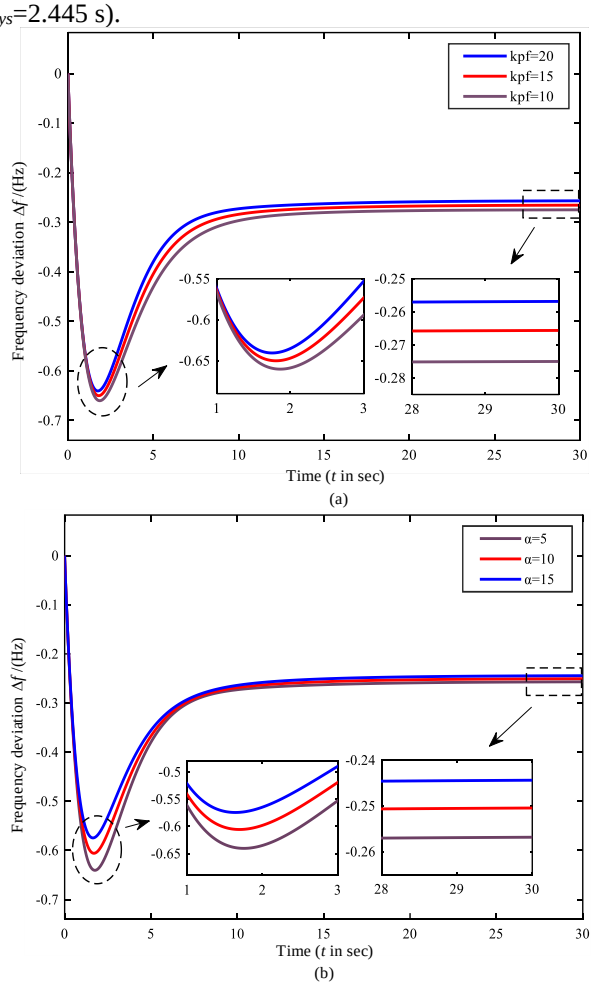

Fig. 9 Primary FR characteristics of power electronic power supply: (a) the effect of k_{pf} on frequency characteristics, (b) the effect of α on frequency characteristics

It can be seen from Fig. 9(a) that the larger the primary FR coefficient k_{pf} of the wind turbine (the active power of the primary FR of the wind turbine increases, and the capability of primary FR is improved), the smaller the absolute value of the maximum frequency deviation and the steady-state frequency deviation. That is, the FR coefficient k_{pf} and the grid frequency is positively correlated. In Fig. 9(b), it can be seen that with the increase of the droop coefficient of flexible HVDC transmission (the increase of the primary FR active power of HVDC transmission), the absolute value of the maximum frequency deviation and the steady-state frequency deviation will be smaller. That is, the FR coefficient α is positively related to the frequency stability of the power grid.

To sum up, when the demand for the minimum inertia of the power grid is insufficient, the frequency characteristics (maximum frequency deviation, steady-state frequency deviation) reach the critical value, then the FR regulation coefficient k_{pf} of the wind turbine and the droop coefficient α of the HVDC transmission can be increased to improve the stable characteristics of the grid frequency,

thereby reducing the demand for minimum inertia in the power system.

4.3.5 Adjustment of the frequency constraints

Taking into account the frequency constraints, the power system considers the safety range of frequency characteristics under the participation of multiple resources in FR to prevent circuit breaker action. When the frequency characteristics of the power grid exceed the limit, that is, exceed the preset action value of the circuit breaker, the problem of insufficient system inertia support capacity occurs at this time. By adjusting the frequency constraints, that is, relaxing the constraint of RoCoF, the constraint of maximum frequency deviation, or the constraint of steady-state frequency deviation, the minimum inertia requirement of the system can be reduced.

The frequency safety domain is defined as the region where the absolute value of the frequency deviation is less than the absolute value of the corresponding point on the frequency curve. It can be seen from Fig. 10 that the frequency characteristics of region 1 and region 2 are different, and region 1 can be regarded as the situation after region 2 has relaxed the frequency constraint. When there is insufficient demand for inertia in region 2, the frequency constraint can be relaxed, that is, the constraint of RoCoF, the constraint of maximum frequency deviation, or the constraint of steady-state frequency deviation can be added.

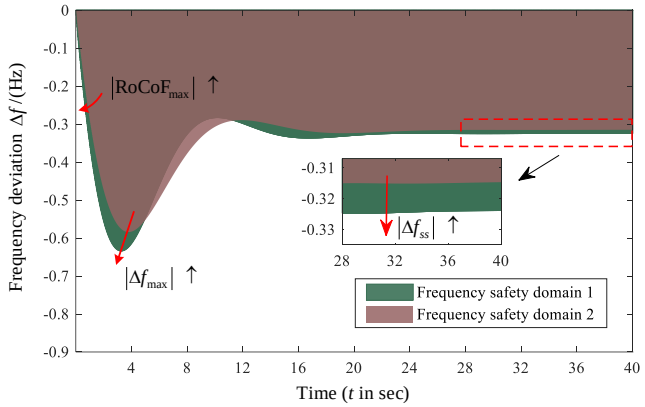

Fig. 10 Primary FR characteristics of power electronic power supply

After the frequency constraints are relaxed, the maximum RoCoF, the maximum frequency deviation, and the absolute value of the steady-state frequency deviation of the system corresponding to domain 1 are larger than those of domain 2, that is, the frequency safety margin of domain 1 is higher.

Taking the constraint of change of frequency as an example, European countries are gradually relaxing the anti-islanding protection threshold of distributed power generation in response to the problem of insufficient inertia in the power system. For example, the UK and Ireland grids have relaxed the anti-islanding thresholds from 0.125 Hz/s and 0.5 Hz/s to 0.5 Hz/s and 1 Hz/s. Combined with Fig. 3, the relationship between the demand for minimum inertia of the power system and the constraint of RoCoF is shown in Fig. 11(ΔP_L=0.1 p.u., D_{sys}=0, R=0.05).

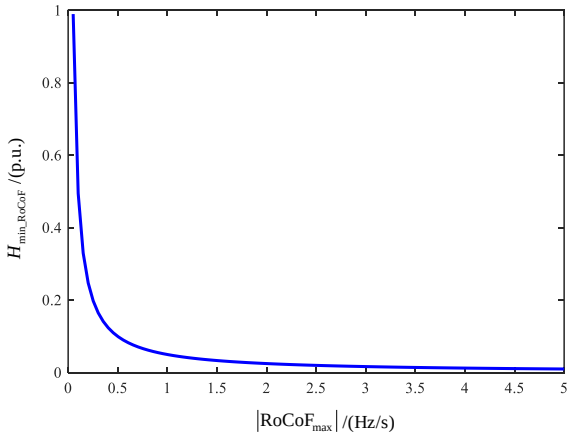

Fig. 11 The relationship between the demand for minimum inertia of the system and the constraint on the RoCoF

According to Fig. 11, it can be seen that with the relaxation of the constraint of RoCoF, the demand for minimum inertia of the system decreases, and the constraint of RoCoF has a nonlinear inverse proportional relationship with the system minimum inertia.

To sum up, based on satisfying the operation safety of the power system, relaxing the constraint of frequency deviation can effectively solve the problem of insufficient system inertia.

4.4. Process of minimum inertia estimation of power system

The estimation of the demand for minimum inertia under different time scales is various. Therefore, according to the transient operation characteristics of the power system, the minimum inertia estimation time scale of the power system under the multi-resource participation FR is divided into a short-time estimation scale and a long-term estimation scale. Using the improved multi-machine SFR model, the source side-load side active power imbalance is defined as the maximum active power disturbance of the system, ΔP_L=ΔP_{max}. Considering the influence of FR resources on the frequency characteristics of the power system, the FR control parameters of different FR units are optimized to improve the frequency stability and also increase the minimum inertia adjustment margin of the system. The main steps are as follows:

1) Calculate the minimum inertia of the power system based on the improved frequency response model of the multi-machine system and the preset constraint of RoCoF, H_{min_RoCoF}.
2) According to the calculated characteristics of system frequency, it is judged whether the constraint of change of the frequency is met. If the frequency change constraints are not met, go to step 3; if so, go to step 8.
3) Reduce the maximum active power disturbance of the power system, so that the maximum frequency deviation meets the constraint of the maximum frequency deviation, ΔP_{max}.
4) Calculate the demand for minimum inertia of the system according to the preset constraint of maximum frequency deviation, $H_{min}^{\Delta f_{max}}$.
5) Determine whether the time scale of the minimum inertia estimation is a long-term estimation scale. If the estimation scale is a long time scale, go to step 6, if not, skip to step 8.

6) Reduce the maximum active power disturbance of the power system, so that the maximum frequency deviation meets the constraint of the maximum frequency deviation, ΔP_{max}.
7) Calculate the demand for minimum inertia of the system according to the preset constraint of steady-state frequency deviation $H_{min}^{\Delta f_{ss}}$.
8) The primary FR control parameters are optimized and adjusted, including the governor differential adjustment coefficient R, the system equivalent damping D_{sys}, the primary FR coefficient k_{pf} of wind turbines, and the droop coefficient of the HVDC transmission α.
9) According to the frequency response model of the multi-machine system after parameter optimization, the minimum inertia of the system H_{min} is simulated and calculated.

The following Fig. 12 shows the minimum inertia estimation process of the power system under the multi-resource participation FR proposed in this paper:

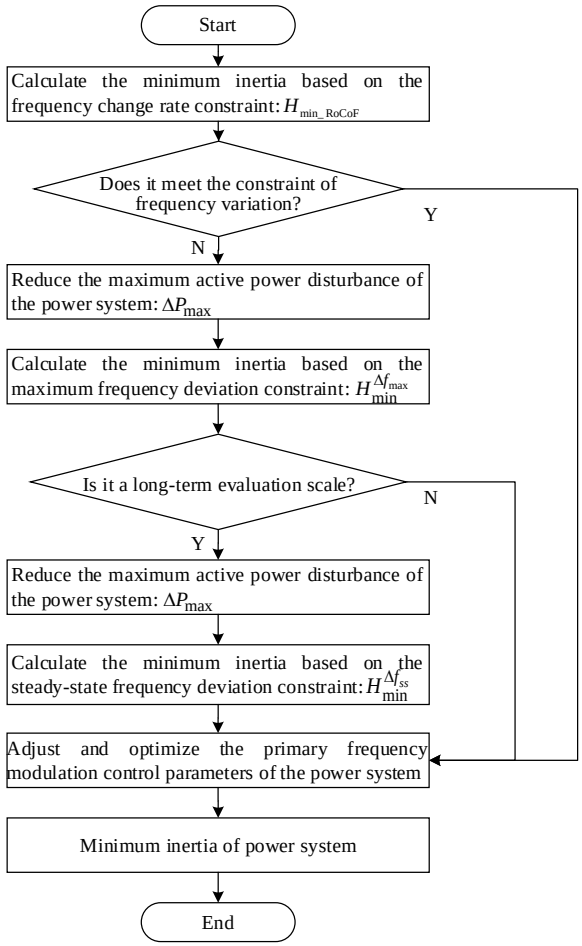

Fig. 12 Minimum inertia estimation process of power system

5. CASE STUDY

To verify the feasibility of the PEPS minimum inertia estimation method considering multi-resource participation in FR proposed in this paper, the PSD-BPA simulation platform is used to analyze the frequency transient stability of the IEEE 10-machine 39-node system.

Based on the existing standard power flow data, the original synchronous generators of BUS 32 and BUS 34 nodes were replaced by equivalent wind farm groups with 440 and 400 double-fed wind turbines respectively. Among them, the model and parameter settings of the replaced double-fed wind turbine are the same: the rated capacity of the double-fed wind turbine is 1.6 MVA, the rated power is 1.5 MW, and the reference voltage is 0.69 kV. In addition, the BUS 1 and BUS 2 bus PQ nodes in the original 10-machine 39-node system were replaced with flexible DC transmission nodes, that is, the original BUS 1-BUS 2 line was replaced with a flexible HVDC transmission line, and the BUS 1 converter station was set as a balance station. The network topology diagram of the improved IEEE 10-machine 39-node system is shown in Fig. 13.

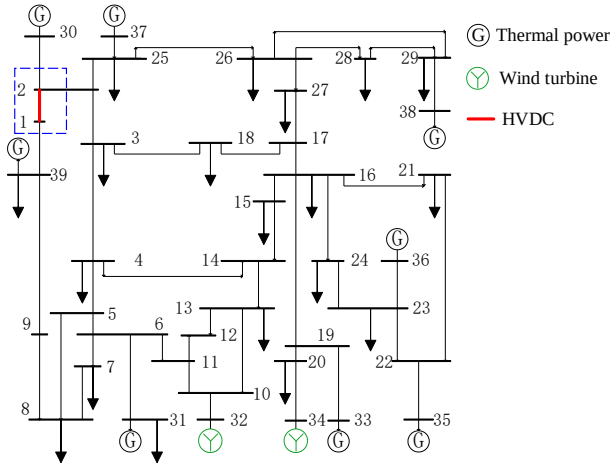

Fig. 13 IEEE 10-machine 39-node power system network topology

In Fig. 13, the total assembly capacity of various types of power supplies in the system is 84266 MW·s, with a total capacity of 4609.65 MVA, and a multi-line load shedding accident occurs when 0s is set. Among them, BUS 31, BUS 33, BUS 35, BUS 36, BUS 37, BUS 38, and BUS 39 cut loads of 20 MW, 35 MW, 40 MW, 20 MW, 10 MW, 20 MW, and 35 MW respectively, with a total of 180MW.

5.1. Validation of the inertia theory

The equivalent inertia time constant of the power system directly affects the frequency response characteristics of the power grid. Therefore, this section studies the traditional system inertia estimation theory and the PEPS inertia theory.

According to (15) (16) (19), the equivalent inertia time constant of the PEPS can be obtained as:

$$H_{sys} = \frac{E_{sys}}{S_{sys}} = \frac{84266\,\text{MW}\cdot\text{s}}{4609.65\,\text{MVA}} = 18.28\,\text{s} \quad (35)$$

In the traditional inertia estimation, only the FR capability provided by synchronous generators such as thermal power is considered, so the kinetic energy does not consider the virtual inertia, and the equivalent inertia time constant of the traditional power system is

$$H_{sys} = \frac{E_{sys}}{S_{sys}} = \frac{74090\,\text{MW}\cdot\text{s}}{4609.65\,\text{MVA}} = 16.07\,\text{s} \quad (36)$$

Based on the improved system frequency response model established in Fig. 1, three scenarios for inertia estimation and analysis are set up:

Case 1: For the topology conditions described in Fig. 14, use the PSD-BPA platform to simulate.

Case 2: Inertia estimation of PEPSs. According to the active power modulation power of the power flow, set the FR coefficient of each FR unit: ρ_R=0.77, ρ_{WF}=0.13, ρ_{DC}=0.1, H_{sys}=18.28 s. The other parameters are shown in Appendix A.

Case 3： Inertia estimation of conventional power systems. The FR coefficient of each FR unit: ρ_R=1 , ρ_{WF}=ρ_{DC}=0, H_{sys}=16.07 s. The other parameters are shown in Appendix A.

Use MATLAB/Simulink to simulate the second and third cases, and compare them with the PSD-BPA simulation results. The frequency characteristic curve of the power system can be obtained, as shown in Fig. 14.

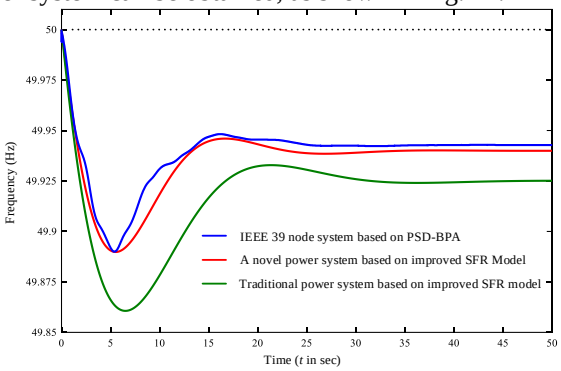

Fig. 14 Comparison of frequency curves under different inertia estimation conditions

The instantaneous frequency values at 0.5 s under the three simulation cases are extracted, which are 49.9806 Hz, 49.9803 Hz, and 49.9759 Hz, respectively, and the respective initial rates of change of the frequency S_{0_sys} are obtained. The frequency characteristic values under the three cases are shown in Tab. 1.

Tab 1. Frequency characteristics of the power system under different inertia estimation conditions

	S_{0_sys}/(Hz/s)	f_{ss_sys}/(Hz)	Δf_{max}/(Hz)
Case 1	-0.0388	49.9428	-0.1100
Case 2	-0.0394	49.9400	-0.1102
Case 3	-0.0482	49.9251	-0.1393

The error formula of this article:

$$\varepsilon = \left| \frac{theoretical\ \ value - actual\ \ value}{actual\ \ value} \right| \times 100\% \quad (37)$$

It can be seen from Fig. 14 and Tab. 1 that, compared with the PSD-BPA simulation data, the frequency response model of the PEPS established based on Fig. 1 shows that the errors of the steady-state frequency and the maximum frequency deviation are $\varepsilon_{\Delta f_{ss\_sys}}$=0.000056 and $\varepsilon_{\Delta f_{max}}$=0.0018, respectively. The error of the two is approximately zero, that is, the curves are almost coincident. Therefore, the frequency response model of the multi-machine system proposed in this paper is feasible.

In addition, according to the simulation data of Cases 2 and 3 and the frequency curve in Fig. 14, it can be seen that the absolute value of the steady-state frequency deviation and the maximum frequency deviation obtained by the system frequency response model under the traditional inertia estimation method is greater than that of the inertia estimation method of the PEPS considering the virtual inertia. Therefore, for the inertia estimation of the PEPS under the multi-resource participation FR, it is necessary to consider both synchronous inertia and virtual inertia.

Based on the above analysis, (18) is used to calculate the inertia expression and the frequency simulation data of case 1 to obtain the equivalent calculation inertia ladder diagram of the power system, as shown in Fig. 15. Using the sliding window technology, the time point t_1 of the active power disturbance is taken as 0 s, and the length of the data sampling interval is 10 frames. That is, v=10, and t_2=t_1+0.08 s can be obtained from formula (12). When t_1=4.2 s, the variance of the equivalent calculated inertia in this sampling interval is the smallest. The specific calculated inertia values are shown in Appendix A.

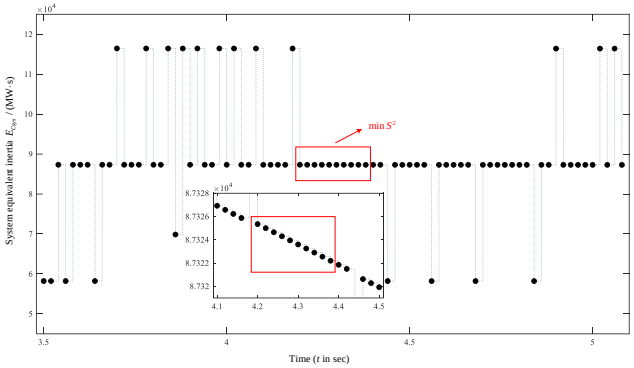

Fig. 15 Ladder Diagram of equivalent calculated inertia of power system

Taking the average value of the calculated inertia sampling data in the above interval, the equivalent calculated inertia of the power system is 87323.78 MW·s. From (37), the calculated inertia error of the PEPS can be obtained as

$$\varepsilon_{E_{Csys}} = \left| \frac{E_{sys} - E_{Csys}'}{E_{sys}} \right| \times 100\% = \left| \frac{84266 - 87323.78}{84266} \right| \times 100\% = 3.63\% \quad (38)$$

To sum up, the equivalent inertia of the PEPS can be calculated using the frequency characteristics of the power system under the multi-resource participation in FR, and the accuracy is high.

5.2. Verification of inertia estimation under RoCoF constraint

It can be seen from Section 5.1 that the error between the inertia estimation results based on the improved multi-machine system frequency response model and the calculation results of the electromechanical transient simulation software is small. Therefore, the inertia estimation method based on the frequency response model of the multi-machine system can reflect the change of the equivalent inertia and frequency response of the power system under the participation of multiple resources in FR.

Considering the inertia estimation under the RoCoF constraint, it is necessary to meet that the absolute value of the initial RoCoF is not greater than the preset critical value index. The parameters of the unit combination should be preset, and the parameters of the units in the system should be determined by simulation. For the convenience of comparative analysis, the power system unit permeability ratio is set unchanged, that is, refer to the data in Section 5.1,

and the specific data are ρ_R=0.77 , ρ_{WF}=0.13 , ρ_{DC}=0.1 , R=0.08. The traditional FR method represented by [30] only considers the inertia support capacity of the traditional synchronous generator set, so the frequency response model of [30] only includes the additional frequency control structure of the traditional synchronous generator. Observe the frequency characteristics of the power system under different FR methods. When the system is subjected to an active power disturbance of 0.11 p.u., the system frequency characteristic curve is shown in Fig. 16.

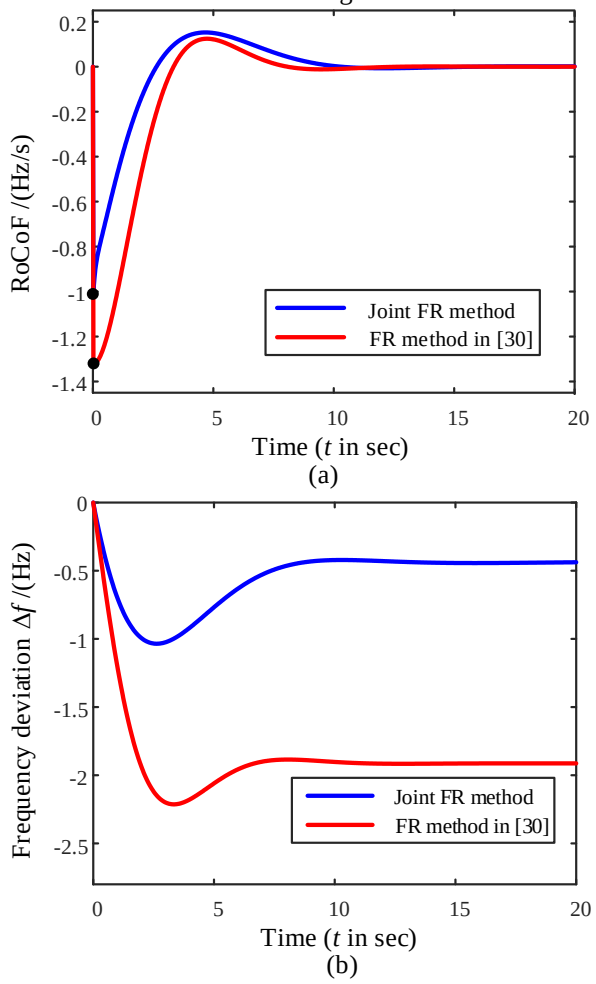

Fig. 16 Frequency characteristic curve of power system: (a) RoCoF, (b) frequency deviation.

Fig. 16(a) is the frequency change rate curve under two different FR modes when H_{sys}=2.7 s is calculated according to (16). When t=0 s, the initial RoCoF under the FR method proposed in this paper is S_{0_sys}=-1 Hz·s^{-1}, while the initial RoCoF of the system under the FR method proposed in [30] is S_{0_sys1}=-1 Hz·s^{-1}. From (8), it can be known that the per-unit value expression of the inertial time constant of the PEPS based on the analysis of the frequency response model is as follows:

$$H_{sys} = \frac{-\Delta P_L}{2S_{0\_sys}} \tag{39}$$

Convert it into an actual value, that is, the actual value of the inertial time constant of the PEPS is expressed as

$$H_{sys} = \frac{-\Delta P_L \cdot f_n}{2S_{0\_sys}} = \frac{-\Delta P_L \cdot 25}{S_{0\_sys}} \tag{40}$$

Based on (40), when the active power disturbance is 0.11 p.u., the calculated values of the inertial time constants of the power system in the above two cases are H_{sys}'=2.75 s, H_{sys1}'=2.08 s, respectively, and the errors obtained according to (30) are $\varepsilon_{H_{sys}'}$=1.85%, $\varepsilon_{H_{sys1}'}$=22.96%, respectively.

From Fig. 16(b), it can be measured that the maximum frequency deviation $\Delta f_{\max}$ and steady-state frequency deviation Δf_{ss_sys} under the two FR methods in this paper and [30] are:

$$\begin{cases} \Delta f_{\max} = -1.035 \text{ Hz}; \ \Delta f_{\max}' = -2.213 \text{ Hz} \\ \Delta f_{ss\_sys} = -0.438 \text{ Hz}; \ \Delta f_{ss\_sys1} = -1.913 \text{ Hz} \end{cases} \tag{41}$$

According to (41), compared with [30], the maximum frequency deviation and steady-state frequency deviation under the frequency situation prediction in this paper are reduced by 1.178 Hz and 1.475 Hz, respectively. Therefore, the multi-resource participation FR mode of the PEPS provides more active inertia support, and the corresponding system frequency characteristics are more stable.

To sum up, the estimation method proposed in this paper is more accurate and has strong feasibility for the inertia estimation under the multi-resource participation FR of the PEPS. And because it is proposed in Section 4.1, in the actual system operation process, since the initial RoCoF is the maximum RoCoF of the power system, the above-mentioned inertial time constant is the minimum inertial time constant. Therefore, when $|\text{RoCoF}_{\max}|$=1 Hz·s^{-1}, the minimum inertia time constant of the power system obtained by the inertia estimation simulation under the RoCoF constraint is $H_{\min\_\text{RoCoF}}'$=2.7 s.

5.3. Validation of inertia estimation under the constraints of frequency deviation

It can be seen from Section 4.2 that in order to prevent the UFLS action of the power system under huge disturbances, it is necessary to ensure that the maximum frequency deviation does not exceed 1 Hz. And because the installed capacity of the IEEE 39 node system is greater than 300 MW, the absolute value of its steady-state frequency deviation does not exceed 0.2 Hz. Set the unit data as follows: ρ_R= 0.77, ρ_{WF}=0.13, ρ_{DC}=0.1, R=0.08. Based on the simulation results in Section 5.2, it can be known that when a disturbance of 0.11 p.u. active power occurs, the minimum inertia of the PEPS under the constraint of the RoCoF meets the condition $H_{\min\_\text{RoCoF}}'$=2.7 s.

Based on the system unit data obtained in Section 5.2, H_{sys}=2.7 s can be calculated according to (16). When the active power disturbance of 0.11 p.u. occurs in the power system, the maximum frequency deviation $\Delta f_{\max}$ and steady-state frequency deviation Δf_{ss_sys} of the power system are -1.035 Hz and -0.438 Hz, respectively, that is, $\Delta f_{\max}$<-1 Hz and Δf_{ss_sys}<-0.2 Hz. Then the system frequency deviation exceeds the frequency deviation constraint value at this time.

5.3.1 Verification of measures to reduce maximum disturbance of active power

Based on the system frequency response model established in Fig. 1, the maximum disturbance of the active power of the system is reduced so that the frequency characteristic curve reaches the condition of frequency constraint. The frequency characteristic curves of the system

under different maximum disturbances of active power are shown in Fig. 17.

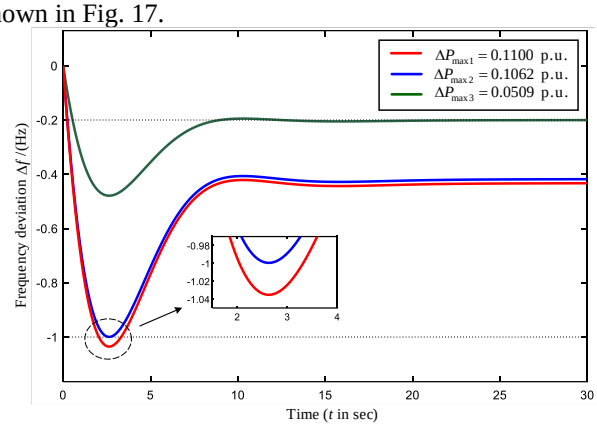

Fig. 17 System frequency curves under different maximum disturbances of active power

The load disturbance is set as the maximum disturbance of active power of the system. Based on the central inertia theory of the frequency response model, and according to (23) and (24), the system inertia can be calculated as the minimum inertia. On the basis of Section 5.2, by reducing the maximum disturbance of active power, the system frequency characteristics can be guaranteed to meet the frequency deviation constraint. It can be seen from Fig. 17 that when the system has the maximum disturbance of active power ΔP_{max1}=0.1100 p.u., the maximum frequency deviation of the power system is Δf_{max1}=-1.035 H and the steady-state frequency deviation Δf_{ss1}=-0.4331 Hz. However, Δf_{max1}<-1 Hz and Δf_{ss1}<-0.2 Hz, which do not meet the constraint of frequency deviation of the system.

In order to meet the constraint of maximum frequency deviation of the system, reducing the maximum disturbance of active power to 0.1062 p.u.. It can be seen from Fig. 18 that Δf_{max2}=-1 Hz and Δf_{ss2}=-0.4182 Hz, only the constraint of maximum frequency deviation is satisfied at this time. Continue to reduce disturbance of the maximum active power of the system to 0.0509 Hz. It can be seen from Fig. 17 that Δf_{max3}=-0.4790 Hz and Δf_{ss3}=-0.2 Hz, which meet the maximum constraint of frequency deviation and the constraint of steady-state frequency deviation.

Therefore, it can be seen that the minimum inertia estimation based on the constraint of frequency deviation can keep the minimum inertia unchanged ($H_{\min}^{\Delta f_{ss}} = H_{\min\_RoCoF}'$=2.7 s) on the basis of the constraint of the RoCoF, and reduce the maximum disturbance of active power to make the minimum inertia meet the constraint of frequency deviation. In addition, according to the simulation results, it is easier to satisfy the maximum constraint of frequency deviation than to meet the constraint of steady-state frequency deviation.

5.3.2 Verification of measures for adjusting conventional primary FR control parameters

When the minimum inertia estimation time scale of the power system is a short time scale, the constraint of frequency deviation only needs to consider the constraint of maximum frequency deviation. This section conducts parameter optimization analysis based on the estimation results in Section 5.3.1. When the disturbance of maximum active power meets ΔP_{max}=0.1062 p.u., the three scenarios are set as:

Case 1: Only increase the equivalent damping D_{sys} of the system;

Case 2: Only reduce the adjustment coefficient R;

Case 3: Increase the equivalent damping D_{sys} of the system and decrease the adjustment coefficient R.

The simulation results are shown in Fig. 18:

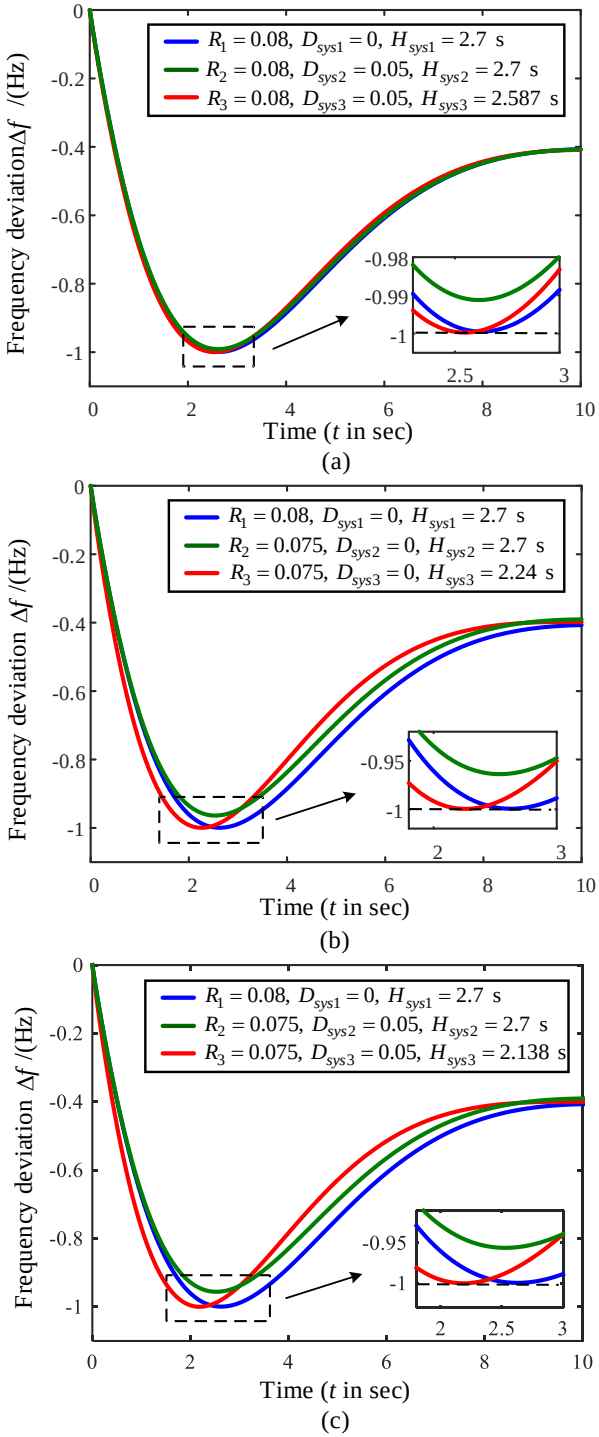

Fig. 18 Frequency characteristic curve after adjusting conventional primary FR control parameters: (a) Case 1, (b) Case 2, (c) Case 3.

Fig. 18(a) is the frequency characteristic curve when only the equivalent damping of the system is adjusted. The equivalent damping coefficient is increased from D_{sys1}=0 to D_{sys2}=0.05, and the maximum frequency deviation is increased from -1 Hz to -0.9912 Hz. In order to meet the constraints of the maximum frequency deviation, reduce the demand for the minimum inertia of the system, and reduce

the constant of equivalent inertia time of the system to 2.587 s. At this time, the maximum frequency deviation of the system is -1Hz. Therefore, increasing the equivalent damping of the system can improve the frequency characteristics and reduce the demand for the minimum inertia of the system.

Fig. 18(b) is the frequency characteristic curve of only adjusting the differential coefficient. The adjustment coefficient is reduced from R_1=0.08 to R_2=0.075, and the maximum frequency deviation is increased from -1 Hz to -0.9637 Hz. To reduce the demand for the minimum inertia, reduce the inertia time constant to 2.24 s, at this time, the maximum frequency deviation is restored to -1 Hz and the maximum frequency deviation constraint condition of the system is satisfied. Therefore, reducing the slack coefficient can increase the system frequency stability and can reduce the demand for the minimum inertia.

Combine the above two conventional primary FR control parameters to optimize the adjustment strategy to improve the system stability characteristics. As shown in Fig. 18(c), the equivalent damping coefficient increases from D_{sys1}=0 to D_{sys2}=0.05, while the adjustment coefficient decreases from R_1=0.08 to R_2=0.075. It can be seen from the simulation results that the maximum frequency deviation increases from -1 Hz to -0.956 Hz. To reduce the demand for the minimum inertia, reduce the inertia time constant to 2.138 s, at this time, the maximum frequency deviation is restored to -1 Hz and the maximum frequency deviation constraint condition of the system is met. Therefore, adjusting the adjustment coefficient and the equivalent damping coefficient of the system at the same time can improve the steady-state characteristics more than the single adjustment of the adjustment coefficient or the equivalent damping, and the minimum inertia of the system is less required.

However, according to (8), it can be seen that due to the reduction of the inertia time constant, the initial RoCoF of the system increases. According to (40), it can be calculated that the initial RoCoF is S_{0_sys}=-1.24 Hz·s^{-1} , which exceeds the constraint of the RoCoF. Therefore, based on the theory in Section 4.3.5, the constraint of the RoCoF can be relaxed to RoCoF$_{max}$=-1.24 Hz·s^{-1} on the basis of satisfying safe operation.

5.3.3 Verification of measures for adjusting FR control parameters of power electronic power supply

The same as the simulation conditions in Section 5.3.2, when the time scale of minimum inertia estimation is a short time scale, the constraint of the frequency deviation only considers the constraint of the maximum frequency deviation. Set the maximum disturbance of active power of the power system to satisfy ΔP_{max}= 0.1062 p.u., and observe the system frequency characteristics and power changes under different power electronic power supply FR control parameters when the system inertia is insufficient, as shown in Fig. 19.

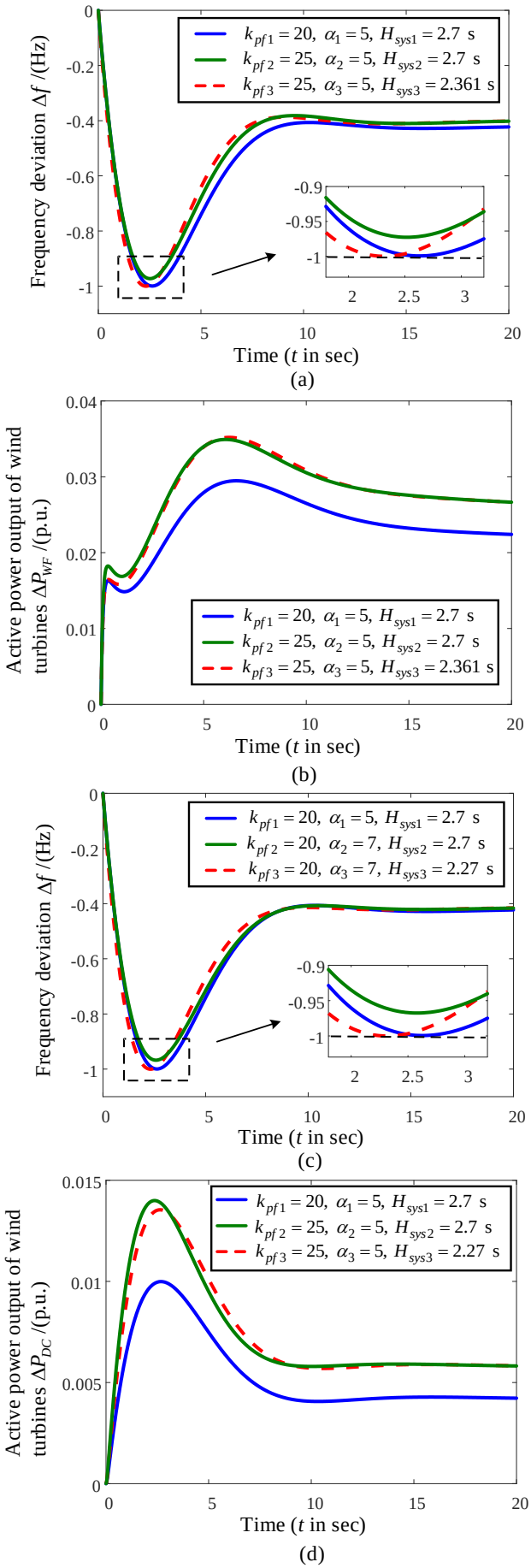

Fig. 19 System frequency characteristic curve under the regulation of power electronic power supply FR control parameters: (a) frequency deviation under different k_{pf}, (b)

FR power of wind units, (c) frequency deviation under different α, (d) FR power of HVDC units

Fig. 19(a) shows the system frequency characteristic curves under different primary FR coefficients of wind turbines, and the corresponding changes in the FR power of wind turbines are shown in Fig. 19(b). According to Fig. 19(a), the primary FR coefficient of the wind turbine is increased from k_{pf1}=20 to k_{pf2}=25, and the constraint of maximum frequency deviation of the system is increased from -1 Hz to -0.9727 Hz. And the maximum value of the primary FR power of the wind turbine is increased from 0.0295 p.u. to 0.0350 p.u., which improves the frequency stability of the system and increases the FR power of the wind turbine. To reduce the demand for the minimum inertia of the system, the inertia time constant is reduced to 2.361 s. At this time, the maximum frequency deviation of the system is -1 Hz, which meets the constraints of the maximum frequency deviation and the primary FR power of the wind turbine does not change. Therefore, increasing the primary FR coefficient of the wind turbine can improve the frequency stability of the system and reduce the demand for minimum inertia.

Fig. 19(c) is the system frequency curve under different droop coefficients of HVDC transmission, and the corresponding FR power of HVDC transmission is shown in Fig. 19(d). According to Fig. 19(c), it can be seen that the droop coefficient of HVDC transmission increases from α_1=5 to α_2=7, the maximum frequency deviation of the system is increased from -1 Hz to -0.9675 Hz, and the maximum FR power of HVDC transmission increases from 9.992×10^{-3} p.u. to 1.4×10^{-2} p.u.. It improves the system frequency stability and increases the FR power of HVDC transmission. Based on this, the inertia time constant of the system is reduced to 2.27 s. At this time, the maximum frequency deviation of the system is -1 Hz, which satisfies the constraint of the maximum frequency deviation. Therefore, increasing the droop coefficient of the HVDC transmission can improve the system frequency stability and reduce the demand for minimum inertia.

However, the initial RoCoF, S_{0_sys}=-1.17 Hz·s^{-1}, can be calculated according to (40), which exceeds the frequency change rate constraint. Therefore, based on the theory in Section 4.3.5, the system constraint of the RoCoF can be relaxed to RoCoF_{max}= -1.17 Hz·s^{-1} on the basis of satisfying safe operation.

6. CONCLUSION

On the basis of considering the diversification of FR resources in the PEPS, this paper proposes an estimation method for the minimum inertia considering the frequency response characteristics. The main conclusions are as follows:

1) Based on the model analysis method, an improved frequency response model of the multi-machine system is established, and the frequency characteristics of the PEPS under multi-resource participation in FR are quantitatively analyzed. According to the frequency characteristics represented by quantization, the improvement measures of the system FR control parameters are proposed when the minimum inertia is insufficient. Through simulation verification, the minimum inertia estimation size of the system can be reduced accordingly after considering the optimization and improvement measures and provides a reference for the adjustment of the system frequency constraint index.

2) Aiming at the diversified development trend of FR resources of PEPS, the theoretical inertia of the power system is expressed in the form of kinetic energy. The real-time inertia of the power system is calculated based on the frequency change characteristics, and the sliding window technology is used to ensure the accuracy of the calculated inertia results. The simulation results show that the application of the sliding window technology makes the error of the calculated inertia to be 3.63%.

3) Given the diversified expansion of FR resources in PEPSs and the complication of FR control methods of FR units, the accuracy of the improved frequency response model of the multi-machine system directly affects the accuracy of the minimum inertia estimation of the system. Therefore, further research is needed to improve the rationality and accuracy of the frequency response model of the PEPS. In addition, with the improvement of the safety action device of the power system, how to adjust the constraint index of frequency change for different power grids needs further discussion.

CONFLICT OF INTEREST

The authors declare no conflict of interest.

DATA AVAILABILITY STATEMENT

The data that support the findings of this study are available from the corresponding author upon reasonable request.

ACKNOWLEDGMENTS

This paper was supported by the National Natural Science Foundation of China under Grant 62073173, the Key Program of National Natural Science Foundation of China under Grant 61933005 and the National Natural Science Foundation of China under Grant 61973151 and 61833011.

REFERENCES

[1] W. Chen, Y. Lei, K. Feng, et al., Provincial emission accounting for CO2 mitigation in China: Insights from production, consumption and income perspectives, Appl. Energy, 2019. 255: p. 113754.
[2] European Commission.: 2030 climate and energy framework existing ambition, 2020.
[3] G. Strbac, D. Papadaskalopoulous, N. Chrysanthopoulos, et al., Decarbonization of Electricity Systems in Europe: Market Design Challenges, IEEE Power Energy Mag., 2021. 19(1): p. 53-63.
[4] U.S. Energy Information Administration.: Annual energy outlook, 2020.
[5] Cai, J, Xu, Q. Capacity value evaluation of wind farms considering the correlation between wind power output and load. IET Gener Transm Distrib. 2021; 15: 1486– 1500.
[6] Xue, Y., Zhang, Z., Hua, W., Wang, G., Xu, Z., Dong, W.: Assessment and enhancement control for small-signal voltage stability of VSC-HVDC systems supplying passive industrial loads. IET Gener. Transm. Distrib. 00, 1– 13 (2023).
[7] Nazari, A.A., Razavi, F., Fakharian, A.: A new power swing detection method in power systems with large-scale wind farms based on modified empirical-mode decomposition method. IET Gener. Transm. Distrib. 00, 1– 12 (2022).
[8] N. Zhao, J. Liu, Y. ai, et al., Power-Linked Predictive Control Strategy for Power Electronic Traction Transformer. IEEE Trans. Power Syst., 2020. 35(6): p. 6559-6571.

[9] N. Soni, S. Doolla, M.C. Chandorkar, Inertia design methods for islanded microgrids having static and rotating energy sources. IEEE Trans. Ind. Appl., 2016, 52(6): 5165-5174.
[10] M. Farrokhabadi, C.A. Cañizares, J.W. Simpson-Porco, et al., Microgrid stability definitions, analysis, and examples. IEEE Trans. Power Syst., 2020, 35(1): 13-29.
[11] H. Gu, R. Yan, T. K. Saha, et al., Zonal Inertia Constrained Generator Dispatch Considering Load Frequency Relief. IEEE Trans. Power Syst., 2020. 35(4): p. 3065-3077.
[12] C. Li, Y. Wu, Y. Sun, et al., Continuous Under-Frequency Load Shedding Scheme for Power System Adaptive Frequency Control. IEEE Trans. Power Syst., 2020. 35(2): p. 950-961.
[13] Z. Ma, C. Shen, F. Liu, et al., Fast Screening of Vulnerable Transmission Lines in Power Grids: A PageRank-Based Approach. IEEE Trans. Smart Grid, 2019. 10(2): p. 1982-1991.
[14] Australian Energy Market Operator: Update report: black system event in South Australia on 28 September 2016. Melbourne, Australia: Australian Energy Market Operation Limited, 2016.
[15] Appendices to the technical report on the events of 9 August 2019. https://www.nationalgrideso.com/document/152351/download.
[16] M. Toulabi, S. Bahrami, A.M. Ranjbar, An Input-to-State Stability Approach to Inertial Frequency Response Analysis of Doubly-Fed Induction Generator-Based Wind Turbines, IEEE Trans. Energy Conversion, 2017. 32(4): p. 1418-1431.
[17] X. Tang, M. Yin, C. Chun, et al., Active Power Control of Wind Turbine Generators via Coordinated Rotor Speed and Pitch Angle Regulation. IEEE Trans. Sustain. Energy, 2019. 10(2): p. 822-832.
[18] N. Tong, X. Lin, Z. Hu, et al., Local Measurement-Based Ultra-High-Speed Main Protection for Long Distance VSC-MTDC. IEEE Trans. Power Delivery, 2019. 34(1): p. 353-364.
[19] J. Zhu, C.D. Booth, G.P. Adam, et al., Inertia Emulation Control Strategy for VSC-HVDC Transmission Systems. IEEE Trans. Power Syst., 2013. 28(2): p. 1277-1287.
[20] L.M. Castro, E. Acha, On the Dynamic Modeling of Marine VSC-HVDC Power Grids Including Offshore Wind Farms. IEEE Trans. Sustain. Energy, 2020. 11(4): p. 2889-2900.
[21] P. Ashton, C. Saunders, G. Taylor, et al. Inertia estimation of the GB power system using synchrophasor measurements. in 2017 IEEE Power & Energy Society General Meeting. 2017.
[22] Y. Zhang, J. Bank, E. Muljadi, et al., Angle Instability Detection in Power Systems With High-Wind Penetration Using Synchrophasor Measurements. IEEE Trans. Emerg. Sel. Topics Power Electron., 2013. 1(4): p. 306-314.
[23] A. Chakrabortty, J.H. Chow, A. Salazar, A Measurement-Based Framework for Dynamic Equivalencing of Large Power Systems Using Wide-Area Phasor Measurements. IEEE Trans. Smart Grid, 2011. 2(1): p. 68-81.
[24] L. Wu, D.G. Infield, Towards an Assessment of Power System Frequency Support From Wind Plant—Modeling Aggregate Inertial Response. IEEE Trans. Power Syst., 2013. 28(3): p. 2283-2291.
[25] H. Gu, R. Yan, T.K. Saha, Minimum Synchronous Inertia Requirement of Renewable Power Systems. IEEE Trans. Power Syst., 2018. 33(2): p. 1533-1543.
[26] S.C. Johnson, D.J. Papageorgiou, D.S. Mallapragada, et al., Evaluating rotational inertia as a component of grid reliability with high penetrations of variable renewable energy. Energy, 2019. 180: p. 258-271.
[27] Q. Shi, F. Li, H. Cui, Analytical Method to Aggregate Multi-Machine SFR Model With Applications in Power System Dynamic Studies. IEEE Trans. Power Syst., 2018. 33(6): p. 6355-6367.
[28] P. Kundur, N.J. Balu, M.G. Lauby, Power system stability and control. New York: McGraw-Hill. 1994: 463-577.
[29] P. Tielens, D.V. Hertem, The relevance of inertia in power systems. Renew. Sust. Energ. Rev., 2016. 55(C).
[30] P.M. Anderson, M. Mirheydar, A low-order system frequency response model. IEEE Trans. Power Syst., 1990. 5(3): p. 720-729.

APPENDIX A:

Simulation parameters:

$D_{sys}=0$, $F_{HP}=0.3$, $T_{RH}=10\text{s}$, $T_G=0.2\text{s}$, $T_{CH}=0.03\text{s}$, $R=0.05\text{s}$, $k_{df}=8$, $T_\beta=4\text{s}$, $k_{pf}=70$, $T_\omega=0.1\text{s}$, $\alpha=5$, $T_{DC}=0.05\text{s}$

4.1 The calculation process of the simulation error:

$$\varepsilon_{\Delta f_{ss\_sys}}=\left|\frac{49.9428-49.9400}{49.9428}\right|\times 100\%=0.000056$$

$$\varepsilon_{\Delta f_{\max}}=\left|\frac{-0.1100-(-0.1102)}{-1100}\right|\times 100\%=0.0018$$

Tab A. Equivalent calculated inertia of power system

Time/(s)	E/(MW·s)
4.20	87325.35
4.22	87325.00
4.24	87324.65
4.26	87324.30
4.28	87323.95
4.30	87323.60
4.32	87323.25
4.34	87322.90
4.36	87322.55
4.38	87322.20